JOURNAL OF GEOPHYSICAL RESEARCH, VOL. 112, A05103, doi:10.1029/2006JA012130, 2007

Click Here for Full Article

Centennial changes in the solar wind speed and in the open solar flux

A. P. Rouillard,[1,2] M. Lockwood,[1,2] and I. Finch[1]

Received 18 October 2006; revised 22 November 2006; accepted 19 December 2006; published 5 May 2007.

[1] We use combinations of geomagnetic indices, based on both variation range and hourly means, to derive the solar wind flow speed, the interplanetary magnetic field strength at 1 AU and the total open solar flux between 1895 and the present. We analyze the effects of the regression procedure and geomagnetic indices used by adopting four analysis methods. These give a mean interplanetary magnetic field strength increase of 45.1 ± 4.5% between 1903 and 1956, associated with a 14.4 ± 0.7% rise in the solar wind speed. We use averaging timescales of 1 and 2 days to allow for the difference between the magnetic fluxes threading the coronal source surface and the heliocentric sphere at 1 AU. The largest uncertainties originate from the choice of regression procedure: the average of all eight estimates of the rise in open solar flux is 73.0 ± 5.0%, but the best procedure, giving the narrowest and most symmetric distribution of fit residuals, yields 87.3 ± 3.9%.

Citation: Rouillard, A. P., M. Lockwood, and I. Finch (2007), Centennial changes in the solar wind speed and in the open solar flux, *J. Geophys. Res.*, *112*, A05103, doi:10.1029/2006JA012130.

1. Introduction

[2] *Lockwood et al.* [1999] used the *aa* geomagnetic index to find that the mean open solar magnetic flux increased during the 20th century, whereas *Feynman and Crooker* [1978] used the same data to infer a rise in the mean solar wind speed at Earth. Four recent developments allow us to investigate these changes further and reconcile these results: (1) the *aa* index has been corrected to allow for intercalibration errors [*Lockwood et al.*, 2007]; (2) *Svalgaard and Cliver* [2005] have developed a new geomagnetic index, termed IDV; (3) *Lockwood et al.* [2007] have developed another new geomagnetic index termed the median index, *m*; (4) *Finch and Lockwood* [2007] have carried out an extensive study (in particular, looking at the effect of data gaps) of the solar wind–geomagnetic field coupling functions used in these extrapolations.

[3] The IDV index is based on the variation of hourly mean geomagnetic data on successive nights and extends back to 1872 (almost the same as the corrected *aa* index, aa_C, which extends back to 1868). The *m* index extends back to 1895 and, like IDV, is based on hourly mean data. Unlike IDV, however, *m* does not discard data when the stations are on the dayside; rather, it treats data from a given station and at a given UT as an independent data series. The hourly means of the horizontal field perturbation for a given station-UT combination are then scaled by linear regression with aa_C and *m* is the monthly median of the 288 data series obtained. Figure 1a shows the variations of the annual means of aa_C, *m,* and IDV. Note that the scaling of the data for each station-UT in terms of aa_C means that the *m* index and aa_C are comparable in magnitude, whereas IDV values are lower: when scaled using a linear regression with aa_C, IDV is similar to *m* but does show some significant differences, as discussed in section 2. Persistent features of aa_C, that are largely missing in IDV and *m*, are peaks during the declining phase of each solar cycle; these correspond to peaks in Sargent's recurrence index, I_{aac}, shown in Figure 2c. The recurrence index is based on the autocorrelation function of aa_C at a lag of 27 days, the mean solar rotation period as seen from Earth [see *Lockwood et al.*, 1999]. These peaks are the effect of corotating fast solar wind streams emanating from long-lived, low-latitude coronal holes, and hence they indicate that the solar wind speed has more effect on aa_C than it does on either IDV or *m*.

[4] The century-scale change in geomagnetic activity is analyzed further in Figure 2. Figure 2a shows both the annual means of aa_C (in red) and the standard deviation of daily values in each year, σ_{aac}. The mean and standard deviation have varied in a similar manner; however, Figure 2b shows that the ratio $\sigma_{aac}/\langle aa_C \rangle$ has declined slightly over the past 150 years and the largest peaks were all before 1960. This ratio is a measure of the fluctuation level, or "relative storminess," of geomagnetic activity and shows that large disturbances in the modern era make a smaller contribution to the average level of geomagnetic activity than they did around 1900. Thus average levels have risen more than the combined effect of the number and intensity of storm events. This is the case for all phases of the solar cycle and hence true of both geomagnetic storms driven by coronal mass ejections (most common at sunspot maximum) and of recurrent storms driven by fast solar wind streams (most common in the declining phase). All the variations shown in Figures 1 and 2 indicate a major change in behavior around 1965, at the end of the solar cycle with the largest-ever amplitude (cycle number 19) and at the start

[1]Rutherford Appleton Laboratory, Chilton, UK.
[2]Also at Solar-Terrestrial Physics Group, Department of Physics and Astronomy, University of Southampton, Southampton, UK.

Copyright 2007 by the American Geophysical Union.
0148-0227/07/2006JA012130$09.00

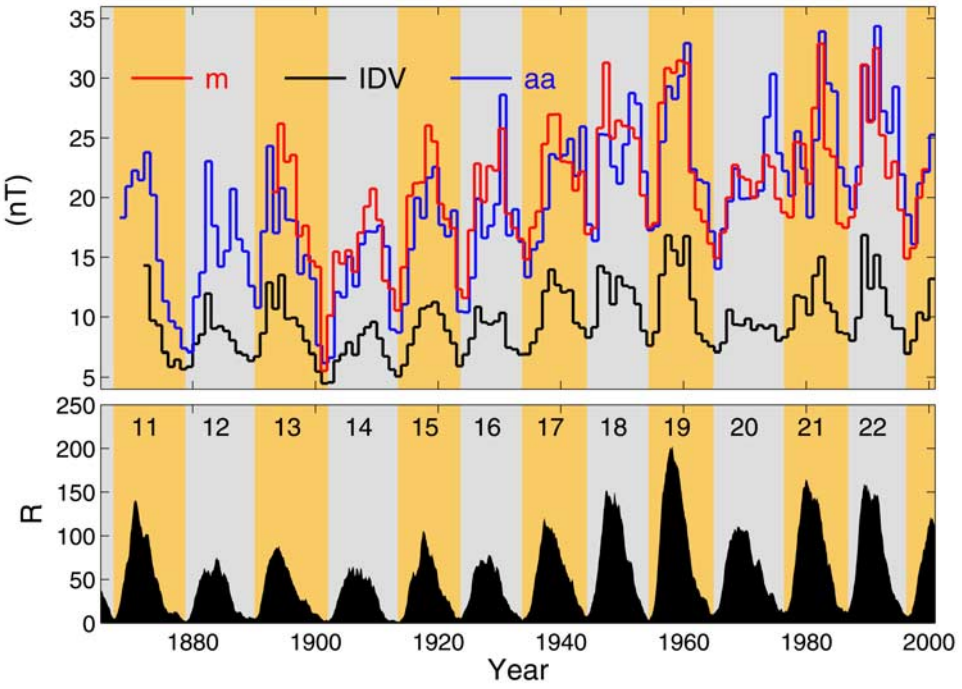

Figure 1. (a) Annual means of geomagnetic indices: the corrected *aa* index, aa_C (blue); the median index, *m* (in red); and IDV (in black). (b) Annual means of the sunspot number, *R*. In both panels the even-numbered solar cycles are shaded grey, the odd cycles orange: cycle numbers are given along the top of Figure 1b.

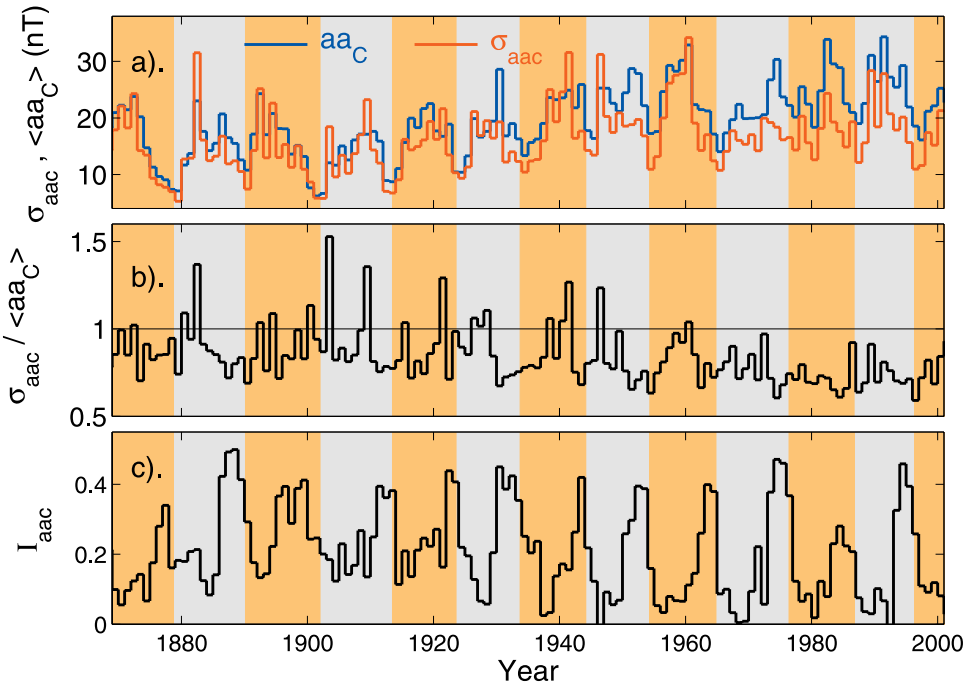

Figure 2. Analysis of the long-term change in the corrected *aa* index, aa_C: (a) The annual means and standard deviations of daily averages of aa_C, $\langle aa_C \rangle$ and σ_{aac}, respectively; (b) the ratio $\sigma_{aac}/\langle aa_C \rangle$; and (c) Sargent's recurrence index derived from aa_C, I_{aac}.

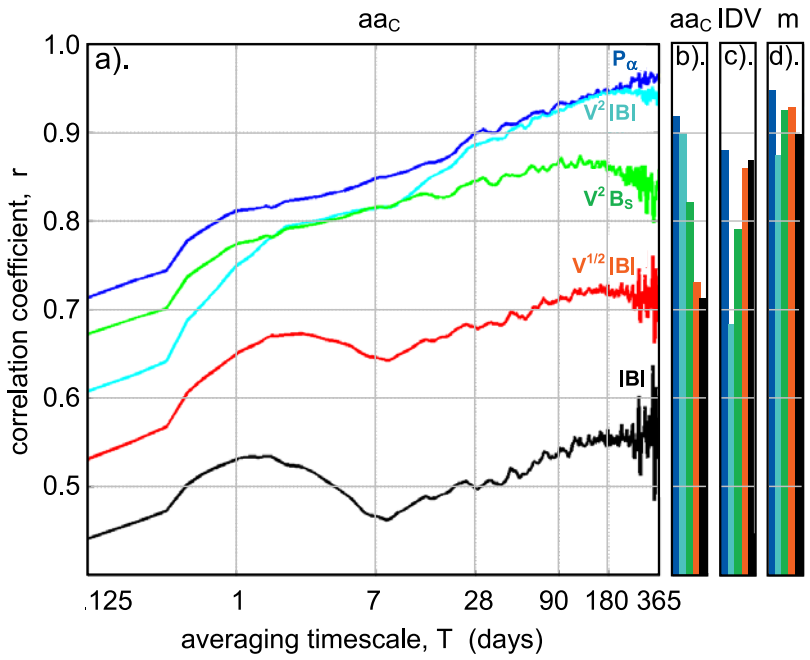

Figure 3. (a) The correlation coefficients between various interplanetary coupling functions and the corrected *aa* index, aa_C, as a function of averaging timescale, *T*. Only coincident (lagged) data are used in Figure 3a and 50% coverage is required for each averaging period. The data are for 1974–2006. (dark blue) $P_\alpha = m_i^{(\alpha+2/3)} M_E^{2/3} N^{(2/3-\alpha)} V^{(7/3-\alpha)} B^{2\alpha} \sin^4(\theta/2)$, where m_i is the mean solar wind ion mass, *N* is the solar wind number density, M_E is the Earth's magnetic moment, θ is the IMF clock angle in the $[Z\text{-}Y]_{GSM}$ frame; (light blue) V^2B; (green) V^2B_s, where $B_s = |B_z|_{GSM}$ if $|B_z|_{GSM} < 0$ and $B_s = 0$ if $|B_z|_{GSM} \geq 0$; (black) *B*; and (red) $V^{0.5}B$ [see *Finch and Lockwood* [2007] for further details]. (b), (c), and (d) The corresponding correlations for annual means (of all available data from 1 January 1974) for aa_C, IDV, and *m*, (for which the best fit exponent α in P_α is 0.3, 0.99, and 0.65, respectively).

of spacecraft observations of the interplanetary medium. The level of all geomagnetic indices dropped at this time (before recovering again) and the recurrence index and relative storminess settled down to the behavior and level seen throughout the space age.

2. Dependence of Geomagnetic Indices on Interplanetary Coupling Functions

[5] *Svalgaard and Cliver* [2005] note that IDV depends on the magnitude *B* of the Interplanetary Magnetic Field (IMF) but is almost independent of the solar wind flow speed *V*, in contrast to the aa_C index that varies with both *V* and *B*. The *m* index shows the same dependence on *B* as aa_C and IDV and shows a weak dependence on *V*. This is demonstrated by Figure 3. A variety of combinations of interplanetary parameters, termed "coupling functions," have been proposed as predictors of geomagnetic activity (see review by *Finch and Lockwood* [2007]). Figure 3a shows the correlation between the corrected aa index, aa_C, and various proposed coupling parameters as a function of averaging timescale, *T*, using the analysis procedure of *Finch and Lockwood* [2007]. All interplanetary data used in this paper are hourly averages from the OMNI-2 data set. These have subsequently been averaged again over the timescale *T* which is varied between 3 hours and 1 year. In Figure 3a, only geomagnetic data with coincident interplanetary observations (allowing for the predicted satellite-to-Earth propagation lag) are used and 50% coverage is required for each averaging interval T for the interplanetary data. It can be seen that the best coupling function for all *T* is P_α, derived by *Vasyliunas et al.* [1982] to be

$$P_\alpha = \mathrm{k} m_i^{(\alpha+2/3)} M_E^{2/3} N^{(2/3-\alpha)} V^{(7/3-\alpha)} B^{2\alpha} \sin^4(\theta/2), \quad (1)$$

where m_i is the mean solar wind ion mass, *N* is the solar wind number density, M_E is the Earth's magnetic moment, and θ is the clock angle of the IMF (with respect to the Z axis) in the ZY plane of the GSM (Geocentric Solar Magnetospheric) reference frame. The correlation of P_α with aa_c is shown as a function if *T* by the dark blue in Figure 1a.

[6] For $T < 1$ month, coupling functions such as P_α which, in addition to *V* and *B*, allow for the IMF orientation (influencing the GSM north-south component, B_z which drives substorm and storm activity) perform significantly better than coupling functions that do not allow for IMF orientation. However, for $T > 1$ month, the IMF orientation effect averages out and Figure 1a shows BV^2 (light blue line) performs almost as well as P_α in correlating with aa_C. Figures 3b, 3c, and 3d show the results for annual means for aa_C, IDV, and *m*, respectively. In these cases, gaps in the interplanetary data series have not been removed from the corresponding geomagnetic data because the fact that they are compiled over different days makes this impossible for *m* and IDV: comparison of the limit $T = 365$ days in Figure 3a

Table 1. Significance of the Differences Between the Best Correlation Coefficients, $r(aa_C, BV^2)$, r(IDV, B), and $r(m, BV^{1/2})$, and Correlations of aa_c, IDV, and m With the Other Two Simple Interplanetary Coupling Functions From the Set of Three (BV^2, B, and $BV^{1/2}$)[a]

	1	2	3
	$r(aa_C, BV^2)$	r(IDV, B)	$r(m, BV^{1/2})$
$r(x, BV^2)$	–	98.85%	95.55%
$r(x, B)$	99.99%	–	50.38%
$r(x, BV^{1/2})$	99.99%	77.22%	–

[a]The geomagnetic index termed "x" is always aa_C for column 1, IDV for column 2, and m for column 3. (So, for instance, the significance of the difference between $r(m, BV^{1/2})$ and $r(m, BV^2)$ is 95.55%). All correlations are for annual mean data. These significances of the differences between two correlations are derived using the modified Fisher-Z (asymptotic) test introduced by *Meng et al.* [1992], which accounts for the persistence in the data and for the fact that the correlation coefficients are obtained from correlated predictors.

with Figure 3b shows that the data gaps in the interplanetary data tend to lower good correlations but raise poor ones. It can be seen that, whereas B correlates with aa_C significantly more poorly than does BV^2 (using the *Meng et al.* [1992] modified Fisher-Z test, the difference between the two correlations is significant at the 99.99% level), B is more highly correlated with IDV than BV^2 (this difference being significant at the 98.85% level). We can readily understand this dependence by noting that aa_C is based on the range of variation of the horizontal field at the ground in 3 hourly intervals and this range can arise either from substorm cycles (driven by IMF B_z in the GSM frame and lasting typically 1–2 hours) and/or from more rapid variations associated with solar wind buffeting, the latter being greater when the mean V is high [*Bowe et al.*, 1990]. On the other hand, IDV is based on hourly means of geomagnetic activity, in which the high-frequency buffeting effect is averaged out. Because the correlation time of V is long (≈30 hours) [*Lockwood*, 2002], high V causes very little difference between hourly means on successive nights, and hence IDV does not respond to high V (*Lockwood*, [2002] showed that the autocorrelation of V at 24 hours lag was as large as 0.65).

[7] The m index correlates best with $V^{0.5}B$. We would expect a lower dependence on V than for aa_C because m, like IDV, employs hourly mean data in which the buffeting effect is averaged out; however, data for a given station-UT are multiples of 24 hours apart, on which timescales V can vary more significantly. The difference between correlations with BV^2 and $BV^{0.5}$ for aa_C is significant at the 99.99% level and for m this figure is 95.55%. A summary of the significance of the differences between correlations is given in Table 1.

3. Determination of IMF Strength and Solar Wind Velocity From Geomagnetic Data

[8] From the above, IDV and aa_C can be used to determine the variations of B and BV^2, respectively, and the variations in both B and V can therefore be derived. *Cliver and Svalgaard* [2006] proposed this technique and applied it to infer a century-scale rise in V, as found by *Feynman and Crooker* [1978]. Similarly, aa_C and m can be used to determine the variations of $BV^{1/2}$ and BV^2, respectively, and estimates of B and V that are independent of IDV can be obtained. Figure 4 shows the scatterplots of annual means of IDV against B (Figure 4a); aa_C against V^2B (Figure 4c); and m against $V^{0.5}B$ (Figure 4e), the best correlations found in Figures 3b, 3c, and 3d, respectively. *Lockwood et al.* [2006] have shown that the assumptions of Ordinary Least Squares (OLS) regression are seriously violated for case a, and in general there are outliers in the annual means of IDV that must be investigated. Specifically, the data are not ''homoscedatic'' (i.e., the variance increases with the fit parameter), the distribution of residuals is not Gaussian, the residuals show systematic drift with the fit parameter, and the regression line is strongly influenced by outliers. These problems are much less severe for either m or aa_C. Hence in addition to OLS, we here also use least squares regression based on Bayesian statistics (BLS). The latter enables us to allow for the fact that a geomagnetic activity index is necessarily an indirect measure of any interplanetary parameter. The mathematical derivation is lengthy but the key result is that least squares minimization is applied to the residuals in the geomagnetic activity index, rather than in the interplanetary parameter, even when predicting the latter (M. Lockwood et al., How large was the rise in open solar flux during the 20th century?: Application of Bayesian Statistics, submitted to *Annales Geophysicae*, 2007). OLS and BLS regression fits for the three data sets are shown in Figure 4 as solid and dashed lines, respectively. The BLS fits are closer to satisfying the assumptions of least squares regression than the OLS fits [*Lockwood et al.*, 2006] as seen from the fit residual distributions plotted in Figures 4b, 4d, and 4e using the same line-type scheme. The errors in the slopes are shown as grey bands on the scatterplots. It can be readily seen that IDV and (to a lesser extent) m have divergent OLS and BLS estimates due to the outliers, whereas regressing aa_C against BV^2 is a very good LS analysis. The best-fit linear regression lines for OLS and BLS can be used to derive the variations of B, BV^2 and $BV^{0.5}$. From these, both B and V are derived in two ways: by combining the fits for (1) IDV and aa_C and (2) m and aa_C, the two sets of parameters whose dependences differ significantly as shown in Table 1.

[9] Figure 5 shows the variations in B obtained in four ways. The blue and green estimates use the OLS regressions for the IDV-aa_C and m-aa_C pairings, respectively, termed B(IDV, aa_C) and $B(m, aa_C)$. The red and black estimates use BLS regressions for B(IDV, aa_C) and $B(m, aa_C)$, respectively. The results show some differences, but all four methods reproduce an average upward drift in 11-year running means of B of 45 ± 4.5 % (mean ± standard error in the mean) between 1902 and 1956. The annual means of the observed values are plotted as black points. Figure 6 shows the estimates of V from OLS (Figure 6a) and BLS (Figure 6c) regressions as well as the distribution of residuals when the derived V are compared to observations (Figures 6b and 6d). As no direct regression fit to V has been made, this is a test of the procedure used. All lines in Figure 6 confirm that mean V has risen (as reported by *Feynman and Crooker* [1978] and *Cliver and Svalgaard* [2006]) and we here find this rise is by 14.4 ± 0.7% between 1903 and 1956. The plots also show the intervals of

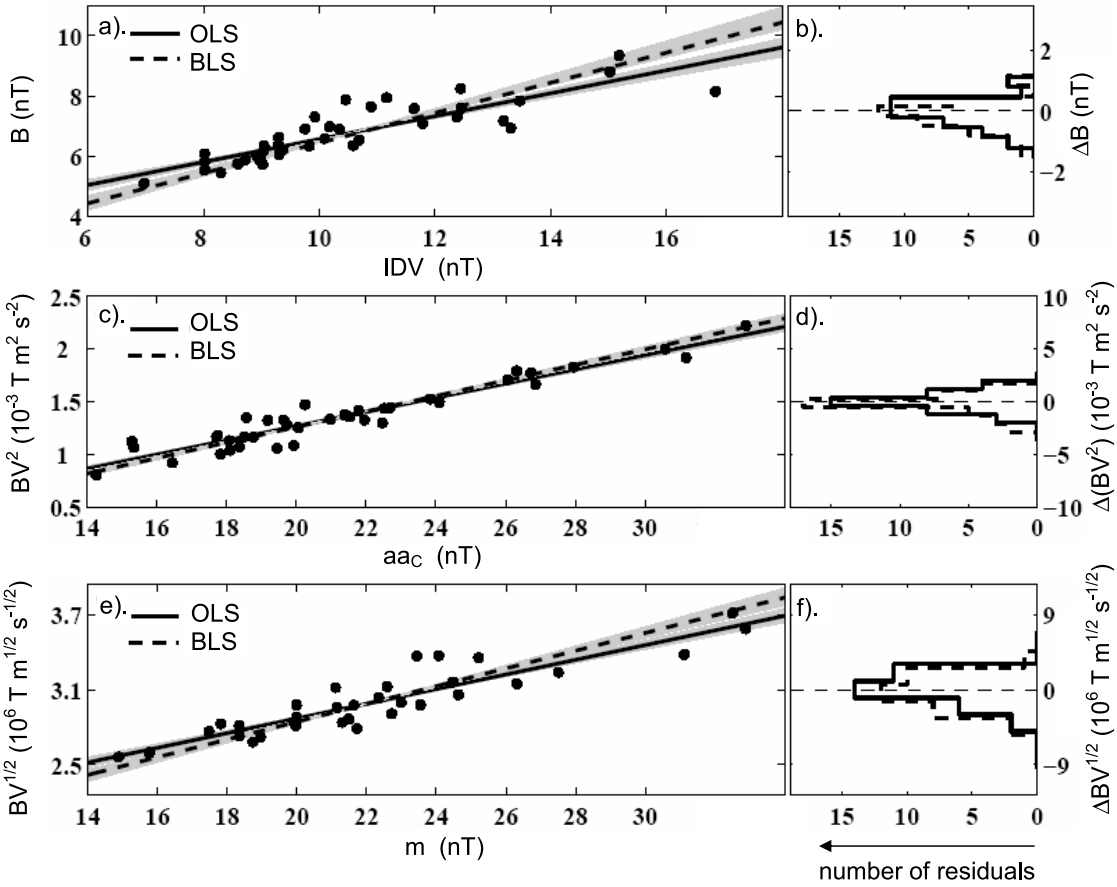

Figure 4. Scatterplots of (a) IDV against B, (c) aa_c against V^2B, and (e) m against $V^{0.5}B$. The regression fits shown employ BLS (solid lines) and OLS methods (dashed lines) and the grey areas give the uncertainties. (b), (d) and (e) The corresponding distributions of the fit residuals.

increased V in the declining phases of sunspot cycles caused by repetitive intersections by the Earth of long-lived coronal hole-extensions that cross the ecliptic (also giving the peaks in I_{aac} seen in Figure 2). The residuals show similar distributions in all cases, but the BLS fits give the most symmetric (and slightly narrower) distributions. A summary of the 11-year running means of V and B for 1903 and 1956 are given in Table 2, as well as the corresponding percentage changes between these 2 years [see *Lockwood et al.*, 2006].

4. Determination of the Open Solar Flux

[10] The Parker theory of the spiral configuration of the average orientation of the solar wind field has been exceptionally successful in reproducing the average IMF direction both in the ecliptic plane [*Balogh et al.*, 1995; *Lockwood et al.*, 2004] and at higher heliographic latitudes [*Forsyth et al.*, 1996]. The theory predicts that the magnitude of the radial field $|B_r| = B\{1 + (r\omega \cos\psi/V)^2\}^{-1/2}$, where r is the heliocentric distance, ψ is the heliographic latitude, B is the IMF magnitude, V is the solar wind speed, and ω is the angular velocity of the Sun. Using the Ulysses result that the radial component of the IMF is independent of ψ, $|B_r| = [F]_{r=1AU}/(2\pi r^2)$, where $[F]_{r=1AU}$ is the (signed)

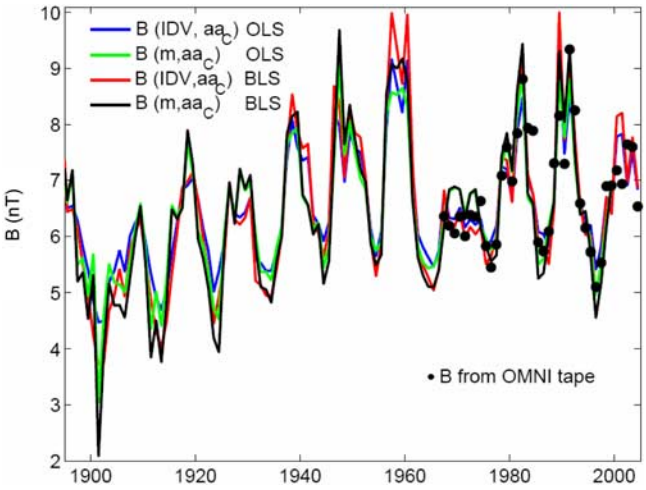

Figure 5. Variations in B derived using the regression fits shown in Figure 4. Regression techniques and geomagnetic indices used are (blue) OLS for IDV and aa_C (for B only IDV is relevant); (green) OLS for m and aa_C; (red) BLS for IDV and aa_C (for B only IDV is relevant); (black) OLS for m and aa_C. Black dots show annual means of observations.

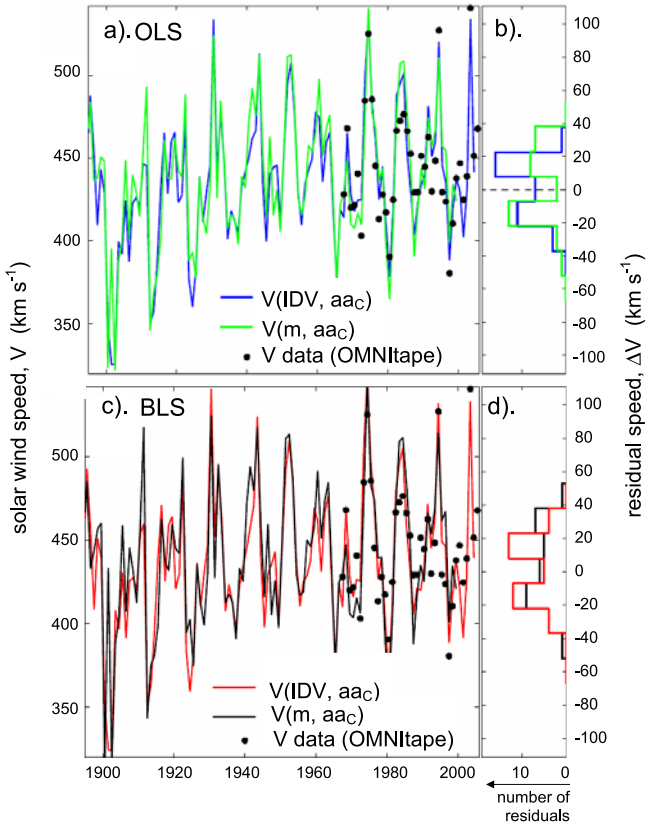

Figure 6. (left) Variations in V derived using the OLS (top) and BLS (bottom) regression fits shown in Figure 4. (right) The distribution of the residuals relative to measured annual means. Colors and symbols are as for Figure 5.

total flux threading the sphere at r = 1 AU [see *Lockwood*, 2004, and references therein]. Hence

$$[F]_{\mathrm{r=1AU}} = 2\pi r^2 B\left\{1 + (r\omega\cos\psi/V)^2\right\}^{-1/2} \quad (2)$$

A measure of the total open solar magnetic flux is the total signed flux derived from potential field source surface (PFSS) extrapolations of solar magnetograms into the solar corona [*Wang and Sheeley*, 2002]. These extrapolations assume that the open magnetic field threads a spherical source surface (of radius 2.5 solar radii) such that it is everywhere orthogonal to that surface, that the corona is current-free, and that the field detected in magnetograms is orthogonal to the photospheric surface. *Lockwood et al.* [2006] showed that the PFSS estimates of the total signed flux agree best with estimates from measurements at 1 AU when the absolute value of the radial field B_r is taken for means of IMF observations for a timescale T between 1 and 2 days:

$$F_S = \left(4\pi r^2 |B_r|_T\right)/2. \quad (3)$$

[11] Figure 7a shows a scatterplot of annual means of F_S for T = 1 day as a function of $[F]_{\mathrm{r=1AU}}$ from hourly means of IMF and solar wind observations for 1967–2005, using equations (3) and (2), respectively. The plot is linear with a correlation coefficient of 0.92 and an OLS regression of F_S = 0.65(±0.03)$[F]_{\mathrm{r=1AU}}$ − 0.69(±0.26) (for fluxes in 10^{14} Wb). Using T = 2 days in equation (2) to derive F_s, this regression becomes F_S = 0.64(±0.03)$[F]_{\mathrm{r=1AU}}$ − 0.89(±0.25). The fit residuals do not show any drift in time (not shown here) and their distribution is approximately Gaussian, as shown by Figure 7b. The difference between F_S and $[F]_{\mathrm{r=1AU}}$ arises from (1) disconnected flux F_d that threads the heliocentric sphere at r = 1AU but not the source surface; (2) distortions from Parker spiral that give multiple crossings of field lines of the sphere at r = 1AU (flux F_m); (3) newly emerged open flux (F_n) that has yet to reach r = 1 AU. In general, $[F]_{\mathrm{r=1AU}} - F_S = \Delta F = (F_d - F_n + F_m)$. Table 2 give results for averaging timescales T of both 1 day and 2 days as ways of estimating and removing the flux ΔF [*Lockwood et al.*, 2007]. Note that the factors in ΔF also contribute to the difference between the long-term changes in B and F_S (the latter being related to $|B_r|_T$ by equation (3)). This is because opposite-polarity B_r is within the averaging interval T cancels, but B is always positive and hence there is no corresponding effect on B. Hence as pointed out by *Lockwood et al.* [2007], although B and F_S are close to being linearly related, they are not proportional. In addition, the use of the regression given in Figure 7a allows for the fact that the ratio B_r/B increases toward unity as the Parker spiral unwinds with increasing V, as predicted by Parker spiral theory.

[12] Using the regression shown in Figure 7a with the derived B and V variations shown in Figures 5–6 yields the open flux F_s. Figures 8a and 8c compare the various estimates with the variation derived by the "recurrence correction method" (RCM) of *Lockwood et al.* [1999], applied to the corrected aa, aa_C (grey area). This RCM method makes use of a relationship between enhanced I_{aac} and aa_C and enhanced mean solar wind speed V, caused by Earth intersecting the fast solar wind emanating from low-latitude coronal holes. The upper and lower edges of the grey area show the upper and lower limits set by the uncertainty in aa_c, as derived by *Lockwood et al.* [2007]. These estimates also use the averaging timescale of T = 1 day and are therefore directly comparable. It can be seen that OLS regressions give lower drift in open flux than BLS ones. The BLS regression using m and aa_c gives a result very close to those from aa_c using the RCM (black line in Figure 8c). Figure 8d shows this combination also does a better job in reproducing the open flux estimated from IMF data, the distribution of residuals being narrower, more symmetric and more Gaussian than for the other methods: we therefore identify this as the optimum of the four procedures. Table 2 presents the changes in open solar flux between 1903 and 1956 inferred by OLS and BLS for the two sets of geomagnetic indices used here, as well as using the RCM of *Lockwood et al.* [1999], with the full range of possible corrections to *aa*. Values for T of 1 and 2 days are given in both cases and various means of the derived percentage changes. The implications of Table 2 are discussed in the next section.

5. Discussion and Conclusions

[13] Table 2 shows that the average open solar flux increase derived from the four procedures is 69.9 ± 6.8%

Table 2. The 11-Year Running Mean Values of V, km s^{-1}, B, nT, and F_S, 10^{14}Wb, for Years 1903 and 1956 Estimated Here From Both Ordinary Least Squares (OLS) and Bayesian Least Squares (BLS) Regressions and Also Using the Recurrence Corrected Method (RCM) of *Lockwood et al.* [1999][a]

			T, days	1903 Value	1956 Value	Change, λ, %
A	OLS	V (IDV, aa_C)	-	391	454	16
B	OLS	V (m, aa_C)	-	401	460	14.7
C	BLS	V (IDV, aa_C)	-	395	451	14.2
D	BLS	V (m, aa_C)	-	406	457	12.6
	Mean V from A-D					14.4 ± 0.7
A	OLS	B (IDV, aa_C)	-	5.4	7.4	37
B	OLS	B (m, aa_C)	-	5.2	7.2	38.5
C	BLS	B (IDV, aa_C)	-	5.0	7.6	52
D	BLS	B (m, aa_C)	-	4.8	7.4	54.2
	Mean B from A-D					45.4 ± 4.5
A1	OLS	F_S (IDV, aa_C)	1	2.8	4.4	57.1
B1	OLS	F_S (m, aa_C)	1	2.7	4.3	59.3
C1	BLS	F_S (IDV, aa_C)	1	2.5	4.5	80.0
D1	BLS	F_S (m, aa_C)	1	2.4	4.4	83.3
	Mean F_S from A1-D1		1			69.9 ± 6.8
E1	RCM	F_S (aa_C)	1	2.1 ± 0.2	4.3 ± 0.2	105 ± 10
A2	OLS	F_S (IDV, aa_C)	2	2.5	4.1	61.9
B2	OLS	F_S (m, aa_C)	2	2.5	4.0	64.3
C2	BLS	F_S (IDV, aa_C)	2	2.3	4.2	87.5
D2	BLS	F_S (m, aa_C)	2	2.2	4.1	91.5
	Mean F_S from A2-D2		2			76.5 ± 7.6
	Mean F_S from A1-D1 & A2-D2		1-2			73.0 ± 5.0
	Mean F_S from D1&D2		1-2			87.3 ± 3.9
E2	RCM	F_S (aa_C)	2	1.9 ± 0.2	4.0 ± 0.2	116 ± 11

[a]The corresponding percentage increases λ between 1903 and 1956 are also shown. Means for all methods are given and for the optimum method (BLS applied to m and aa_c, shown in the rows labeled D1 and D2 for the timescale T of 1 and 2 days, respectively). All rows labeled A give the results of OLS regression analysis using IDV and aa_C; rows labeled B give the results of OLS regression analysis using m and aa_C; rows labeled C and D are the corresponding results for BLS analysis. For the open solar flux F_S, the results also depend on the averaging timescale T employed and, for example, A1 and A2 are the results for OLS regression analysis using IDV and aa_C with T of 1 and 2 days, respectively. Results using the RCM of *Lockwood et al.* [1999] are given in rows E1 and E2 (for T of 1 and 2 days, respectively).

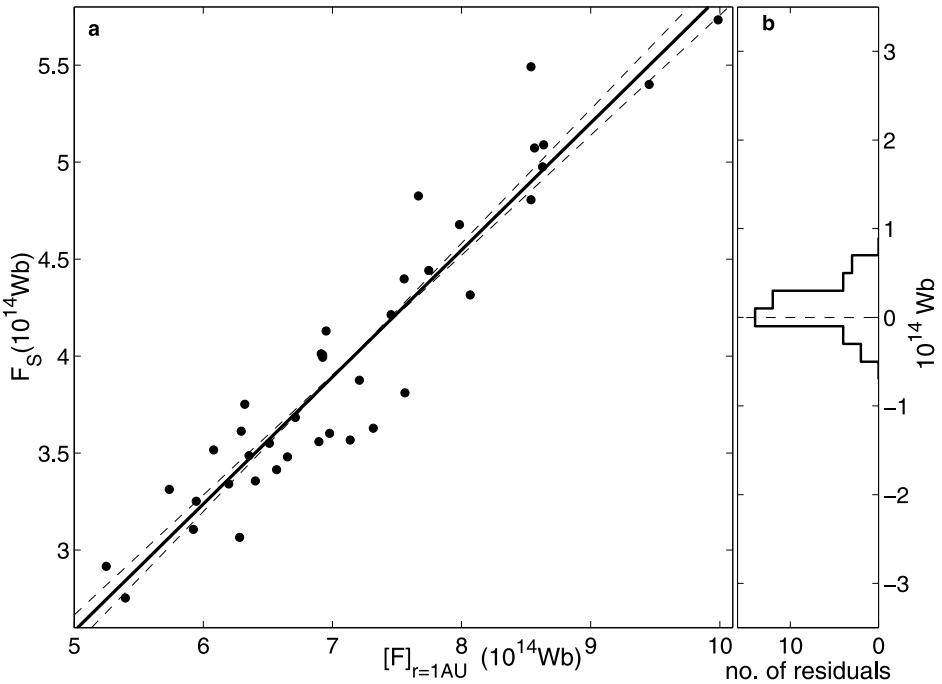

Figure 7. (a) Scatterplot and regression fit for annual means of the (signed) open solar flux F_S as a function of the (signed) flux threading r = 1AU, $[F]_{r=1AU}$ from hourly means of IMF and solar wind observations for 1967–2004, using equations (3) and (2), respectively. In this example, a timescale T = 1 day is used. The correlation coefficient is 0.92 (significant at the 99.9% level). The dotted lines show the effect of the estimated maximum errors in the slope on the best-fit line. (b) The distribution of best-fit residuals (thick line). The residuals are close to Gaussian, validating the use of the estimated error in the slope and intercept.

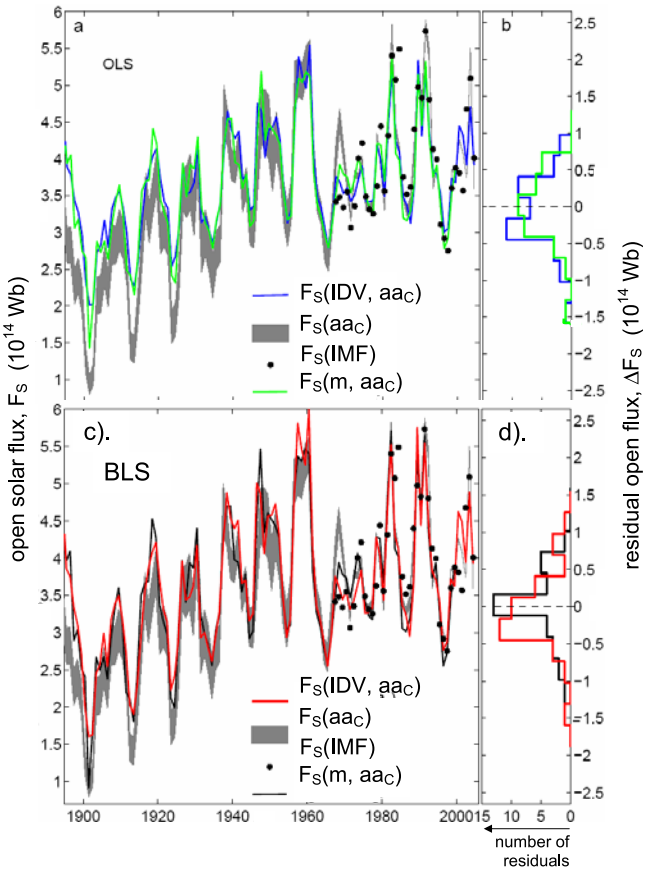

Figure 8. (left) The variation of (signed) open solar flux F_s derived from B and V variations using the regression shown in Figure 7 for absolute values taken on means for an averaging timescale $T = 1$ day. The area shaded grey is the range of possibilities using the corrected *aa* index, aa_C, from the RCM procedure of *Lockwood et al.* [1999] for the same T. Black dots show observed annual means from IMF data (from equation (2), also for the same T). (right) The corresponding distributions of residuals. The upper two plots are for OLS, the lower two for BLS regressions. Line colors and symbols are as in Figure 5.

between 1903 and 1956 for $T = 1$ day, rising to 76.5 ± 7.6% for $T = 2$ days. Using the BLS regression with m and aa_C, which gives the best fit to the IMF observations, these rises become 83.3% and 91.5% and, given this is the range of uncertainty in the optimum T, we here find 87.3 ± 3.9% to be the best estimate. *Svalgaard and Cliver* [2005] discuss the change in B and not the total open flux, and their estimate of "~25%" is directly comparable to the corresponding average of 45.4 ± 4.5% for the change in B that we derive here. An increase in open solar flux, as inferred by *Lockwood et al.* [1999], is here confirmed by all methods. The relationship between the derived increases in the open solar flux and the mean solar wind speed at Earth can be understood from the empirical law derived by *Wang and Sheeley* [1990]. This law relates the large/low expansion of open magnetic flux tubes between the photosphere and the coronal source surface to slow/fast solar wind speeds in the heliosphere [*Wang and Sheeley*, 1990, 1997]. On annual timescales, the accumulation of open field lines in coronal holes should force lower expansion rates of magnetic flux tubes. This in turn should increase the probability of the Earth intersecting the fast solar wind, thereby raising the average measured solar wind speed.

[14] The above estimates of the percentage change in open solar flux can be directly compared to the 105 ± 10% and 116 ± 11% rises obtained by applying the RCM method of *Lockwood et al.* [1999] to the corrected aa, aa_c, for T of 1 and 2 days, respectively. The differences arise out of the long-term drift in V revealed by Figure 6. The method of *Lockwood et al.* [1999] assumed that the relationship of B and B_r over the past 150 years had been as it was during the past four solar cycles, i.e., it did not allow for the effect of a long-term change in V on the Parker spiral "garden-hose" angle. By using a regression of the type shown in Figure 7, we generalize this assumption to allow for changes in V by assuming that Parker spiral theory has remained valid for annual means over the 150 years. The above numbers show that the 14% rise in V has reduced the estimated change in open solar flux by of order 15%.

[15] Finally, we stress that the magnitude of the rise in open solar flux derived here has been predicted by several numerical models. *Solanki et al.* [2002] used a simple continuity model to reproduce the rise and fuller numerical modeling of the emergence and evolution of solar flux by *Lean et al.* [2002], *Wang and Sheeley* [2002], *Wang et al.* [2005], and *Schrijver et al.* [2002] has also reproduced the change. These models show that the open solar flux variation is what one should expect because of the enhanced flux emergence in active regions, associated with increased peak sunspot numbers, over the same period [*Foster and Lockwood*, 2001] (see Figure 1b) and the mean lifetime of the open flux. The best estimate of the magnitude of the rise (derived here to be 87.3 ± 3.9%) is very similar indeed to that produced by the numerical simulations: *Wang et al.* [2005] obtained a cycle-averaged increase of ~83% over the first half of the 20th century and the various simulations presented by *Schrijver et al.* [2002] gave rises between 70% and 90%. Analysis of cosmogenic isotope abundances reveals decreases in the production of both ^{14}C and ^{10}Be that are highly anticorrelated with the rise in open solar flux. *Lockwood* [2003] showed that variations of the ^{10}Be isotope (from the Dye-3 Greenland ice core) and of the ^{14}C production rate (derived from observed abundances in tree rings using a two-reservoir model) both show a strong and significant anticorrelation with the open solar flux deduced from *aa*. Further evidence for the century-scale drift in open flux has been found from the ^{44}Ti cosmogenic isotope found in meteorites [*Taricco et al.*, 2006]. The relationship between the decreases in ^{10}Be and the increase in open flux has been investigated quantitatively by *McCracken et al.* [2004] and *Caballero-Lopez et al.* [2004]. We note that the Caballero-Lopez et al.'s most-likely estimate of a 40% change in B agrees very well with the 45% change in B derived here (consistent with the 87% open flux variation) but will be a slight underestimate as it does not allow for the effect of the associated rise in V.

[16] **Acknowledgments.** A.P.R. thanks both Kalevi Mursula and Georgeta Maris for inviting him to the exciting "Second International Symposium on Space Climate" held in Sinaia, Romania, September 2006

when some key ideas of this paper were formulated. The geomagnetic data used in this paper were obtained through the World Data Center C1, UKSSDC, Chilton, UK. The interplanetary data were obtained from the OMNIWeb Space Physics Data Facility at the NASA Goddard Space Flight Center. This work was funded on a PPARC Rolling Grant.

[17] Amitava Bhattacharjee thanks Tuija I. Pulkkinen and another reviewer for their assistance in evaluating this paper.

References

Balogh, A., E. J. Smith, B. T. Tsurutani, D. J. Southwood, R. J. Forsyth, and T. S. Horbury (1995), The heliospheric magnetic field over the south polar region of the Sun, *Science*, *268*, 1007–1010.

Bowe, G. A., M. A. Hapgood, M. Lockwood, and D. M. Willis (1990), Variability of solar wind number density, speed and dynamic pressure as a function of the interplanetary magnetic field components: A survey over two solar cycles, *Geophys. Res. Lett.*, *17*, 1825–1828.

Caballero-Lopez, R. A., H. Moraal, K. G. McCracken, and F. B. McDonald (2004), The heliospheric magnetic field from 850 to 2000 AD inferred from ^{10}Be records, *J. Geophys. Res.*, *109*, A12102, doi:10.1029/2004JA010633.

Cliver, E. W., and L. Svalgaard (2006), The solar wind during grand minima, paper presented at ISSC-2: Long-Term Changes in the Sun and their Effects in the Heliosphere and Planet Earth, Int. Symp. on Space Clim., Sanai, Romania.

Feynman, J., and N. U. Crooker (1978), The solar wind at the turn of the century, *Nature*, *275*, 626–627.

Finch, I. D., and M. Lockwood (2007), Solar wind-magnetosphere coupling functions on timescales of 1 day to 1 year, *Ann. Geophys.*, *25*, 495–506.

Forsyth, R. J., A. Balogh, T. S. Horbury, G. Erdös, E. J. Smith, and M. E. Burton (1996), The heliospheric magnetic field at solar minimum: Ulysses observations from pole to pole, *Astron. Astrophys.*, *316*, 287–295.

Foster, S. S., and M. Lockwood (2001), Long-term changes in the solar photosphere associated with changes in the coronal source flux, *Geophys. Res. Lett.*, *28*, 1443–1446.

Lean, J. L., Y.-M. Wang, and N. R. Sheeley Jr. (2002), The effect of increasing solar activity on the Sun's total and open magnetic flux during multiple cycles: Implications for solar forcing of climate, *Geophys. Res. Lett.*, *29*(24), 2224, doi:10.1029/2002GL015880.

Lockwood, M. (2002), Relationship between the near-Earth interplanetary field and the coronal source flux: Dependence on timescale, *J. Geophys. Res.*, *107*(A12), 1425, doi:10.1029/2001JA009062.

Lockwood, M. (2003), Twenty-three cycles of changing open solar magnetic flux, *J. Geophys. Res.*, *108*(A3), 1128, doi:10.1029/2002JA009431.

Lockwood, M. (2004), Solar outputs, their variations and their effects of Earth, in *The Sun, Solar Analogs and the Climate*, pp. 107-304, Springer, New York.

Lockwood, M., R. Stamper, and M. N. Wild (1999), A doubling of the sun's coronal magnetic field during the last 100 years, *Nature*, *399*, 437–439.

Lockwood, M., R. B. Forsyth, A. Balogh, and D. J. McComas (2004), Open solar flux estimates from near-Earth measurements of the interplanetary magnetic field: comparison of the first two perihelion passes of the Ulysses spacecraft, *Ann. Geophys.*, *22*, 1395–1405.

Lockwood, M., A. P. Rouillard, I. Finch, and R. Stamper (2006), Comment on "The IDV index: Its derivation and use in inferring long-term variations of the interplanetary magnetic field strength" by Leif Svalgaard and Edward W. Cliver, *J. Geophys. Res.*, *111*, A09109, doi:10.1029/2006JA011640.

Lockwood, M., D. Whiter, B. Hancock, R. Henwood, T. Ulich, H. J. Linthe, E. Clarke, and M. A. Clilverd (2007), The long-term drift in geomagnetic activity: calibration of the aa index using data from a variety of magnetometer stations, *Ann. Geophys.*, in press.

McCracken, K. G., F. B. McDonald, J. Beer, G. Raisbeck, and F. Yiou (2004), A phenomenological study of the long-term cosmic ray modulation, 850-1958 AD, *J. Geophys. Res.*, *109*, A12103, doi:10.1029/2004JA010685.

Meng, X. L., R. Rosenthal, and D. B. Rubin (1992), Comparing correlated correlation coefficients, *Psych. Bull.*, *111*, 172–175.

Schrijver, C. J., M. L. DeRosa, and A. M. Title (2002), What is missing from our understanding of long-term solar and heliospheric activity?, *Astrophys. J.*, *577l*, 1006–1012.

Solanki, S. K., M. Schüssler, and M. Fligge (2002), Secular variation of the Sun's magnetic flux, *Astron. Astrophys.*, *383*, 706–712.

Svalgaard, L., and E. W. Cliver (2005), The IDV index: Its derivation and use in inferring long-term variations of the interplanetary magnetic field strength, *J. Geophys. Res.*, *110*, A12103, doi:10.1029/2005JA011203.

Taricco, C., N. Bhandari, D. Cane, P. Colombetti, and N. Verma (2006), Galactic cosmic ray flux decline and periodicities in the interplanetary space during the last 3 centuries revealed by ^{44}Ti in meteorites, *J. Geophys. Res.*, *111*, A08102, doi:10.1029/2005JA011459.

Vasyliunas, V. M., J. R. Kan, G. L. Siscoe, and S.-I. Akasofu (1982), Scaling relations governing magnetospheric energy transfer, *Planet. Space Sci.*, *30*, 359–365.

Wang, Y.-M., and N. R. Sheeley (1990), Magnetic flux transport and the sunspot-cycle evolution of coronal holes and their wind streams, *Astrophys. J.*, *365*, 372–386.

Wang, Y.-M., and N. R. Sheeley (1997), The high-latitude solar wind near sunspot maximum, *Geophys. Res. Lett.*, *24*, 3141–3144.

Wang, Y.-M., and N. R. Sheeley (2002), Sunspot activity and the long-term variation of the Sun's open magnetic flux, *J. Geophys. Res.*, *107*(A10), 1302, doi:10.1029/2001JA000500.

Wang, Y.-M., J. Lean, and N. R. Sheeley (2005), Modeling the Sun's magnetic field and irradiance since 1713, *Astrophys. J.*, *625*, 522.

I. D. Finch, Space Science Department, Rutherford Appleton Laboratory, Chilton, Didcot, Oxfordshire OX11 0QX, UK. (i.d.finch@rl.ac.uk)

M. Lockwood and A. Rouillard, Solar-Terrestrial Physics Group, Department of Physics and Astronomy, University of Southampton, University Road, Southampton SO17 1BJ, UK. (m.lockwood@rl.ac.uk; AlexisRouillard@yahoo.co.uk)